Magnetic energy fluxes in close-in star-planet systems

A. Strugarek[1,2], A. S. Brun[2], S. P. Matt[3] and V. Réville[2]

[1]Université de Montréal, C.P. 6128 Succ. Centre-Ville, Montréal, QC H3C-3J7, Canada
email: `strugarek@astro.umontreal.ca`
[2]CEA-Saclay, IRFU/SAp, Gif-sur-Yvette, France.
[3]Department of Physics & Astronomy, University of Exter, EX2 4QL, UK

Abstract. Magnetic interactions between a close-in planet and its host star have been postulated to be a source of enhanced chromospheric emissions. We develop three dimensional global models of star-planet systems under the ideal magnetohydrodynamic (MHD) approximation to explore the impact of magnetic topology on the energy fluxes induced by the magnetic interaction. We conduct twin numerical experiments in which only the magnetic topology of the interaction is altered. We find that the Poynting flux varies by more than an order of magnitude when varying the magnetic topology from an aligned case to an anti-aligned case. This provides a simple and robust physical explanation for on/off enhanced chromospheric emissions induced by a close-in planet on time-scales of the order of days to years.

1. Introduction

The diversity of masses, sizes and orbits of known exoplanets has lead the scientific community to intensely explore the broad range of interactions that can exist between planets and their host stars (see Cuntz *et al.* 2000). Recently, Shkolnik *et al.* (2008) reported on/off chromospheric emissions for five different star-planet systems that seemed to be related to the orbital period of the close-in planet. The surprising lack of X-ray emissions of WASP-18 (Pillitteri *et al.* 2014) is also postulated to be related to its short-period orbiting planet. Although close-in planets do not seem to induce systematic emissions features (Miller *et al.* 2015), these occasional intriguing observations require further theoretical investigations. Furthermore, radio and UV emissions from star-planet magnetic interactions are also intensively researched today (Grießmeier *et al.* 2007; Fares *et al.* 2010; Lecavelier des Etangs *et al.* 2013; Turner *et al.* 2013), as any detection would give us observational constraints on the magnetic field of such close-in planets (see, *e.g.* Zarka 2007; Vidotto *et al.* 2015).

In addition to tidal interactions (e.g. Mathis *et al.* 2013), planets orbiting inside the stellar wind Alfvén radius can magnetically interact with their host (Ip *et al.* 2004; Cohen *et al.* 2010; Strugarek *et al.* 2014). The latter are a promising candidate to explain the aforementioned observations (*e.g.* Kopp *et al.* 2011), based on the interaction of an hypothetical planetary magnetosphere with the stellar magnetospheric wind. Among the star-planet interaction (SPI) models that have been developed, MHD simulations combine state of the art numerical models of cool stars magnetospheres and winds (Matt *et al.* 2012; Réville *et al.* 2015) with simplified models of planets (e.g., Cohen *et al.* 2014; Strugarek *et al.* 2014, and references therein). These global, dynamical models enable us to assess the effects of SPI in a self-consistent manner, by taking into account the full interaction channel from the planetary magnetosphere down to the lower stellar corona.

In a recent paper (Strugarek *et al.* 2015), we have developed MHD simulations of

magnetic star-planet interactions in three dimensions. We address here the magnetic energy carried alfvénically through the so-called *Alfvén wings*, which are systematically excited by the interaction of an orbiting planet (with a magnetosphere) with the ambient magnetized wind. We focus in particular on the key role magnetic topology plays in determining the shape and strength of the Alfvén wings. We first briefly describe our methodology in Section 2, and quantify the Poynting flux through the Alfvén wings in Section 3. We conclude in Section 4 by showing that changes in magnetic topology can very simply provide an on/off mechanism for the enhanced emissions induced by a close-in planet.

2. Three-dimensional models of star-planet magnetic interaction

We model magnetic star-planet interactions with global numerical simulations using the ideal MHD approach. We use the modular code PLUTO (Mignone *et al.* 2007) to solve the MHD equations with a standard HLL Riemann solver coupled to a second-order Runge-Kutta method for the time integration. The soleinoidality of the magnetic field is enforced with a constrained transport method (see Strugarek *et al.* 2015). We use a cartesian grid in which a star and a planet are treated as internal boundary conditions. A magnetized stellar wind is imposed at the stellar surface. A given hypothetical magnetic field is enforced at the planetary boundary. We solve the MHD equations in the orbital rotating frame, in order to fix the planet on the simulation grid. The star is positioned at the center of the simulation grid. It hence remains fixed in the grid as well (the stellar rotation rate is corrected to account for the orbital rotating frame). The simulations are computed on a $490 \times 355 \times 355$ grid, with a resolution of $0.03\,R_\star$ at the stellar boundary and a resolution of $0.06\,R_P$ (here we consider $R_P = 0.1\,R_\star$) in the vicinity of the planet.

The central star is a typical cool star with a coronal temperature of 10^6 K, and a relatively strong magnetic field such that the Alfvén speed v_A at the base of the corona is equal to the escape velocity $v_{\rm esc}$ (for details see Strugarek *et al.* 2015). The star slowly rotates ($v_{\rm rot} = 3.03\,10^{-3}\,v_{\rm esc}$) and its wind is characterized by a large average Alfvén radius $\langle R_A \rangle = \sqrt{\dot{J}/\Omega_\star \dot{M}} \sim 18\,R_\star$ (see, e.g., Matt *et al.* 2012).

The close-in planet is considered to have a circular orbit (close-in planets are generally thought to be tidally-locked) and is located inside the Alfvén surface of the wind at $R_o = 5\,R_\star$. The relative velocity between the rotating wind and the orbiting planet is smaller than the local Alfvén speed of the wind as well, which ensure a sub-alfvénic SPI. We assume that the planet possess an intrinsic dipolar magnetic field sufficiently large to retain a magnetosphere. The surface planetary magnetic field is chosen to be 10 times larger than the wind magnetic field at the planetary orbit. We choose to neglect any kind of planetary outflows (see Matsakos *et al.* 2015, for a complete discussion about such outflows) to focus on the effect of magnetic topology on the star-planet interaction itself. In the following, we consider the two opposite cases of aligned and anti-aligned (compared to the orientation of the wind magnetic field) dipolar planetary fields.

We illustrate those two configurations in Figure 1 with a three-dimensional representation of the interaction. In the aligned case (left panel), the magnetic topology allows the polar magnetic field lines of the planet (gray lines) to connect with the wind magnetic field lines (coloured lines). In the anti-aligned case (right panel), the planetary magnetosphere remains closed due to the incompatible topology of the two magnetic fields. Parallel current $J_{||} = \nabla \times \mathbf{B} \cdot \hat{\mathbf{b}}/\mu_0$ ($\hat{\mathbf{b}}$ is the unit vector along the magnetic field $\mathbf{B}$) are shown by the red/blue (positive/negative) transparent volume renderings in the two cases. The parallel currents delimit the extent of the Alfvén wings (Neubauer 1998; Saur
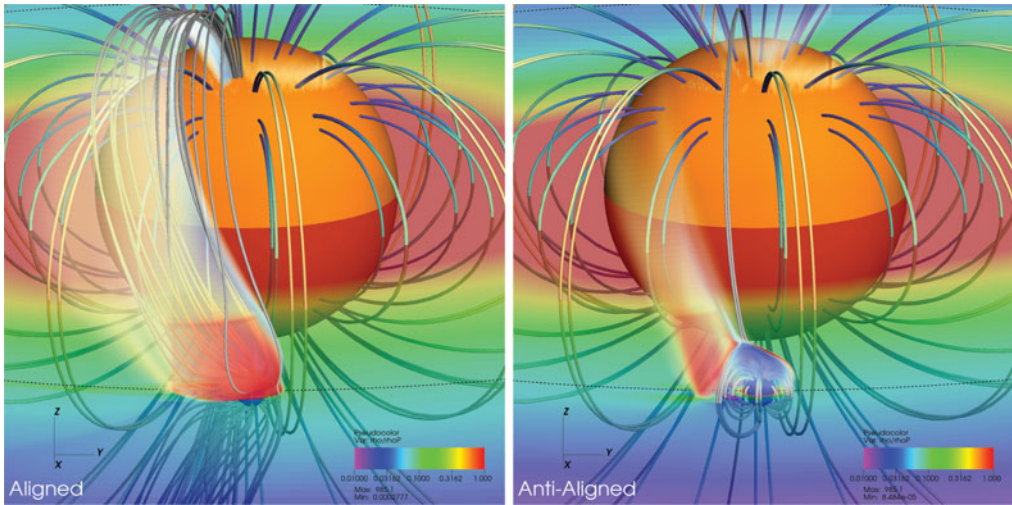
Figure 1. 3D renderings of the two star-planet interaction simulations. The stellar wind magnetic field lines are color-coded with the magnetic field strength, and the magnetic field lines connected to the planet are shown in gray. The stellar surface is represented by the orange sphere, and the planetary surface by the blue sphere. On the orbital plane the orbit is labeled by the black dashed line, and the logarithm of the density is shown by the transparent colormap. The transparent blue/red volume rendering shows the strong (negative/positive) parallel currents delimiting the Alfvén wings.

et al. 2013; Strugarek *et al.* 2015). Two symmetric wings extend above and below the orbital plane, we only show the upper wing here. We recall that only the orientation of the planetary field has been changed between the two cases, leaving all the other parameters untouched. Nevertheless, we immediately see that the Alfvén wing dramatically changes: the characteristic size and strength of the parallel current structures are much larger in the aligned case. We now quantify how this structural change affects the energy fluxes carried through the Alfvén wings.

3. Alfvén wings and Poynting flux

The alfvén wings are composed of superposed alfvénic perturbations which propagate along the Alfvén characteristics $\mathbf{c}_A^{\pm} = \mathbf{v}_0 \pm \mathbf{v}_A$, where $\mathbf{v}_0 = \mathbf{v}_{\text{wind}} - \mathbf{v}_K$ is the differential velocity between the wind velocity and the keplerian velocity of the planet, and $\mathbf{v}_A = \mathbf{B}/\sqrt{4\pi\rho}$ is the local Alfvén speed. The Poynting flux along each Alfvén wing can be evaluated by

$$S_a = \frac{c\mathbf{E} \times \mathbf{B}}{4\pi} \cdot \frac{\mathbf{c}_A^{\pm}}{\left|\mathbf{c}_A^{\pm}\right|}, \tag{3.1}$$

where the electric field $c\mathbf{E} = -\mathbf{v} \times \mathbf{B}$ in the ideal MHD approximation. We calculate the Poynting flux in the inertial reference frame to mimic what a distant observer would see. We display in Figure 2 the Poynting flux along the c_A^- Alfvén wing (above the orbital plane). On the right panels we display an horizontal cut at $z = 3\,R_p$ on which the Alfvén wing cross-section is identified by a black contour. The colormaps represent the Poynting flux S_a normalized to the expected theoretical value $v_0 B_w^2/4\pi$ (see Saur *et al.* 2013). The projected planet diameter and its orbit are symbolized by the blue circle and dashed line. The Alfvén wing acts in both cases as an obstacle to the flow $\mathbf{v}_0$ (gray arrows), which
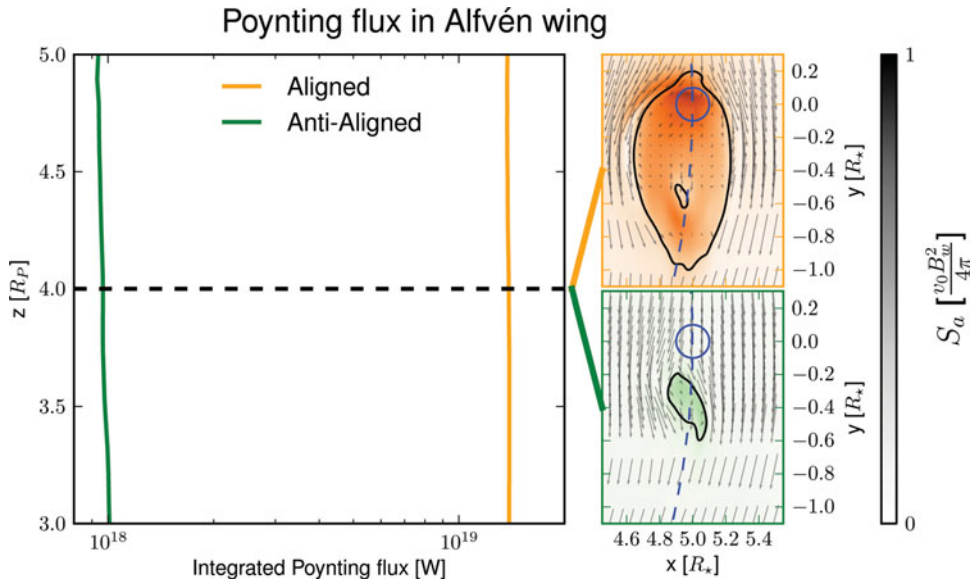
Figure 2. Poynting flux along the c_A^- Alfvén wing in the aligned (orange) and anti-aligned (green) cases. The right panels show a colormap of the normalized Poynting flux inside the wing, which is delimited by the black contour, at $z = 4\,R_p$ above the orbital plane. The flow $\mathbf{v}_0$ is represented by the gray arrows. On the left panel the Poynting flux is integrated over horizontal cross-sections of the Alfvén wing and displayed as a function height above the orbital plane.

means that it actually orbits along with the planet. The cross-section area of the wing is significantly smaller in the anti-aligned case, and the wing extends to about $10\,R_p$ along the orbital direction in the aligned case.

The modification of the Alfvén wing cross-section between the two cases has an important consequence on the magnetic energy flux through the wing. The integrated Poynting flux inside the wing is shown on the left panel for both cases, as a function of height above the orbital plane. We first note that it remains relatively constant, as a result of flux conservation throughout the wing and showing that the energy is transported into the stellar corona without significant dissipation at this height. As expected, the total Poynting flux dramatically changes between the two configurations: it is more than an order of magnitude higher in the aligned case. Let us now consider a more realistic case of a close-in star-planet system. Stars generally possess a complex large-scale magnetic topology, which means that a planet will interact with a varying relative magnetic topology along its orbit. The magnetic field of cool stars is furthermore expected to reverse polarity (as it is the case for the Sun) over periods years to tens of years, which will significantly affect the amount of magnetic energy channeled through the Alfvén wings. Hence, changes in the magnetic topology of the interaction are expected to occur on short (order of days to years) time-scales in close-in star-planet systems, even if the planetary magnetic field is simple and non-varying. As a result, the magnetic energy channeled by the interaction will also vary by a least an order of magnitude on such time-scales. Our results suggest that observed enhanced emissions related to a close-in planet are expected to be very variable on short time-scales (the so-called on/off mechanism) due to this simple topological effect.

Our simulations are adimensionalized, which allows each case to represent several physical systems. As an example, once the Alfvén speed at the base of the corona is fixed

(see Section 2), one simulation can represent several physical cases by varying together the stellar wind magnetic and its density. We hence are free to choose the density normalization, which must adequately reflect the physical star-planet systems we want to simulate. Here we assume that the stellar wind mass-loss rate is equivalent to the solar wind mass-loss rate, which sets our density normalization. We then compute the total Poynting flux in physical units [W], as reported on the left panel of Figure 2. In the aligned case we obtain a Poynting flux higher than 10^{19} W, slightly less in magnitude than a typical solar flare. Nevertheless, the Poynting flux gives only an upper estimate of any observable signal, as further work is needed to clarify how much of this input energy can be converted into coronal and chromospheric emission.

4. Conclusions

We have demonstrated how magnetic topology affects close-in star-planet interactions using three-dimensional global numerical simulations. We developed twin simulations of such systems in which we only changed the orientation of the planetary field. We showed that the magnetically aligned case develops much stronger Alfvén wings than the anti-aligned case. As a result, the magnetic energy channeled through the wings varies by more than an order of magnitude between the two configurations. For moderate stellar $(B_\star \simeq 10$ G) and planetary $(B_P \simeq 1$ G) magnetic fields, the close-in planet magnetic interaction leads to energy leads to Poynting fluxes of the order of 10^{19} W in the aligned case.

Real stars posses much more complex magnetic fields than the simple dipolar configuration we considered here. In reality close-in planets are likely to interact with different local magnetic configurations along their orbit. As a result, the energy channeled through the wings is expected to vary on relatively short time-scales (of the order of days to years), providing a robust and simple physical explanation for the on/off emissions observed in real close-in star-planet systems (see, *e.g.* Shkolnik *et al.* 2008). Nevertheless, dedicated 3D simulations tackling the dynamical aspects of a planet orbiting in a non-homogeneous corona are needed. In addition, the time-scale on which the equilibrated configurations modelled in this work establish depends on the resistivity of the magnetospheric plasma of the planet, and on its reconnection efficiency with the stellar wind magnetic field. The numerical model presented in this work provides a solid basis for further, more realistic studies of star-planet magnetic interactions in which these dynamical aspects could be explored.

References

Cohen, O., Drake, J. J., Glocer, A., *et al.* 2014, *ApJ*, 790, 57
Cohen, O., Drake, J. J., Kashyap, V. L., Sokolov, I. V., & Gombosi, T. I. 2010, *ApJ*, 723, L64
Cuntz, M., Saar, S. H., & Musielak, Z. E. 2000, *ApJ*, 533, L151
Fares, R., Donati, J.-F., Moutou, C., *et al.* 2010, *MNRAS*, 406, 409
Grießmeier, J. M., Zarka, P., & Spreeuw, H. 2007, *A&A*, 475, 359
Ip, W.-H., Kopp, A., & Hu, J.-H. 2004, *ApJ*, 602, L53
Kopp, A., Schilp, S., & Preusse, S. 2011, *ApJ*, 729, 116
Lecavelier des Etangs, A., Sirothia, S. K., & Gopal-Krishna, Zarka, P. 2013, *A&A*, 552, 65
Mathis, S., Alvan, L., & Remus, F. 2013, EAS Publications Series, 62, 323
Matsakos, T., Uribe, A., & Königl, A. 2015, *A&A*, 578, A6
Matt, S. P., MacGregor, K. B., Pinsonneault, M. H., & Greene, T. P. 2012, *ApJL*, 754, L26
Mignone, A., Bodo, G., Massaglia, S., *et al.* 2007, *ApJS*, 170, 228
Miller, B. P., Gallo, E., Wright, J. T., & Pearson, E. G. 2015, *ApJ*, 799, 163

Neubauer, F. M. 1998, *Journal of Geo. Res.*, 103, 19843

Pillitteri, I., Wolk, S. J., Sciortino, S., & Antoci, V. 2014, *A&A*, 567, A128

Réville, V., Brun, A. S., Matt, S. P., Strugarek, A., & Pinto, R. F. 2015, *ApJ*, 798, 116

Saur, J., Grambusch, T., Duling, S., Neubauer, F. M., & Simon, S. 2013, *A&A*, 552, 119

Shkolnik, E., Bohlender, D. A., Walker, G. A. H., & Collier Cameron, A. 2008, *ApJ*, 676, 628

Strugarek, A., Brun, A. S., Matt, S. P., & Réville, V. 2014, *ApJ*, 795, 86

—. 2015, *ApJ*, 815, 111

Turner, J. D., Smart, B. M., Hardegree-Ullman, K. K., *et al.* 2013, *MNRAS*, 428, 678

Vidotto, A. A., Fares, R., Jardine, M., Moutou, C., & Donati, J.-F. 2015, *MNRAS*, 449, 4117

Zarka, P. 2007, *Plan. and Space Sci.*, 55, 598